

Active Triangulation Rangefinder Design for Mobile Robots

Nicholas Pears and Penelope Probert

Department of Engineering Science
Oxford University

19, Parks Road, Oxford, OX1 3PJ, ENGLAND.

Abstract

Design considerations are presented for rangefinders which employ active triangulation. The geometric tradeoffs for conventional triangulation geometries are identified, and the way in which these can be minimised using a synchronized scanning approach is described. We compare the performance of the charge-coupled device (CCD) and lateral-effect photodiode (LEP) as active rangefinder image sensors and discuss the benefits and drawbacks of different optical sources (lasers and LEDs). We predict the performance of a large depth of field laser/LEP sensor and compare real results with theoretical prediction.

1 Introduction

The development of good sensors is a central area of robotics research. Sensors which can provide accurate and reliable information at a high bandwidth are essential for efficient and robust execution of robotic tasks. This fact has motivated the development of a new ranging sensor, which is based on active triangulation, and which is being developed to work over the short-medium ranges required for manoeuvring in a cluttered environment. For a lateral-effect diode (LEP) based sensor, we show that we can maintain a range accuracy of 1% at bandwidths suitable for real-time planning. This accuracy compares well with other rangefinders available at comparable cost. In addition, we have extended the application range of LEPs, which are normally used at fixed ranges and small depths of field, or with retroreflective targets.

This paper is partly tutorial, resulting from a programme of work to determine the best configuration for an obstacle avoidance rangefinder. This discussion is of relevance to anyone involved in using or constructing range sensors. At each stage, we describe the design choices for our sensor. Later sections predict and summarize the accuracy achieved.

In the following section, we review briefly some popular optical ranging techniques. Comprehensive reviews of ranging techniques can be found in [1], [4] and [8]. Section 3 defines the specification of a wide field of view, large depth of field ranging sensor. Subsequently, the design tradeoffs in the construction of a standard active triangulation geometry are elucidated, and the way in which synchronised scanning can minimize these performance tradeoffs is described. In section 5, the lateral-effect photodiodes is described and, in the following

section, its performance is compared with that of the CCD. Section 7 compares coherent and incoherent optical sources in active ranging applications with particular emphasis on laser eye safety. In section 8, the theoretical performance of an LEP based ranging system is calculated and compared with real results.

2 Optical ranging techniques

2.1 Passive Vision Techniques

Passive vision provides the most comprehensive source of sensory information; but the projection of a 3-D scene into a 2-D image engenders ambiguity, making the 3-D reconstruction of the scene difficult. The human eye-brain visual system performs 3-D reconstruction from a pair of colour intensity images; thus, although the hardware for processing information is very different and the existence of algorithmic parallels between the machine vision and psychophysical vision worlds is debatable, there is proof (by existence) that excellent performance can be achieved. This, in part, has motivated research in areas of passive machine vision which exploit the visual depth cues of stereo disparity, camera and object motion ("structure from motion"), shadows and occlusions, surface reflectance ("shape from shading"), and texture gradients.

The practical difficulty of passive machine vision techniques in the real-time execution of robotic tasks is the high bandwidth of data which is expensive to process. Often the use of passive vision is precluded, since processing time limits the bandwidth of range information below that required for a specific real-time task.

2.2 Active triangulation

Active triangulation techniques have been used extensively [2, 3, 10, 11] to provide a workable solution to the 3-D imaging problem. An attractive feature of all such systems is that instances of a featureless scene, as encountered by passive stereo systems, are eliminated. Scene coverage can be achieved either by scanning a spot or line stripe, or by projecting a pattern of dots or lines on to the area of interest.

2.2.1 Scanning techniques

In scanning systems, either a light spot, or a light stripe expanded from a spot using a cylindrical lens, is scanned. Using

such techniques, there is no correspondence problem, since only one portion of the scene is examined at any time.

A light stripe is attractive for applications in which the scanned beam is accessible to the human eye, since it presents a much smaller eye hazard for a given amount of laser power output. Stripe projection, however, can only be used with 2-D segmented detectors such as the CCD. In addition, stripe systems have poor immunity to ambient light because the signal power is dispersed over a large image. This means that a longer integration time is required to obtain the same signal level as a spot system and, as a result, the noise due to ambient light will be increased.

2.2.2 Projected pattern techniques

Active triangulation systems have been developed in which a pattern of dots or lines are projected in order to cover all parts of the scene simultaneously. With this approach, the bandwidth of the sensor is increased and the need for potentially expensive and complex scanning is obviated at the expense of reintroducing the correspondence problem. Some systems have tackled this correspondence problem or *node labelling problem* using coding of line thickness, space or colour. Others have utilised two or more different viewpoints of the pattern or have constructed trinocular systems consisting of one camera and two projectors [3].

2.3 Optical radar

Optical radar (lidar) is a time of flight method. For the relatively short distances involved with autonomous vehicle operation, the speed of light is too great to measure the round trip of light pulses. Instead, the phase relationship between an amplitude modulated light beam (laser, or collimated LED as in [6]) and its reflection is used to calculate the round-trip time. This ranging method is more practical than triangulation in outdoor environments where, at large ranges, triangulation becomes inaccurate. In addition, the missing parts problem, which is a characteristic of any stereo/triangulation system, is eliminated, since the transmitted and received beams are co-axial. However, over short ranges, such systems are generally of low accuracy when compared with active triangulation systems.

3 Sensor specification

Consideration of the various ranging techniques presented in the robotics literature has led us to believe that active triangulation schemes offer the greatest potential for acquiring the short-medium range data required for autonomous vehicle obstacle avoidance.

A prototype ranging device using active triangulation and a synchronised scanning technique is under development. At present, our development consists of a scanning camera head, interface electronics, and a software package which runs on a PC. The functions of the software include calibration of the sensor, statistical analysis of range measurements, and the presentation of range images. Ultimately, the sensor will be interfaced

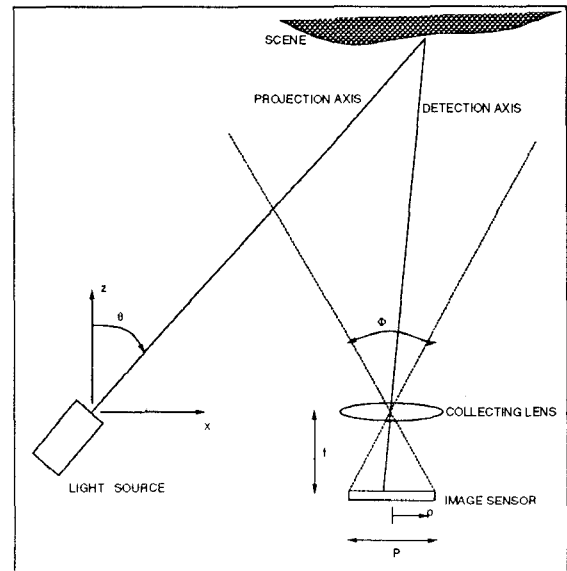


Figure 1: One dimensional active triangulation geometry

to a transputer and will be used in the implementation of an obstacle avoidance controller for a Robuter mobile platform.

The performance specification of our obstacle avoidance sensor is given below in order to illustrate, in further sections, our choice of triangulation geometry and image sensor.

- horizontal scan angle: 40 degrees
- samples per horizontal scan: 100
- vertical scan angle/stripe divergence angle: 30 degrees (-25 - +5 degrees)
- samples per vertical scan: 10
- minimum range: 0.4m
- maximum range: 2.5m
- time for full scan: 0.1-1s
- laser safety: class I (exempt)

4 Triangulation geometries

4.1 Conventional geometries

The basic geometry of active triangulation is shown in fig. 1. It can be seen that the axis of detection is determined by object range along the projection axis, and the position of the principal point of the light collecting lens. Simple geometric analysis of fig. 1 can be used to reveal the tradeoffs in the design of triangulation systems. If we assume that the range of the object is large compared with the focal length of the collecting lens, then the focal plane is at a distance f from the principal point of the lens and:

$$z = \frac{fd}{p + f \tan \theta} \quad (1)$$

$$x = z \tan \theta \quad (2)$$

In the limit, the ratio of image resolution to range resolution is defined as the triangulation gain (G_p) and, from (1), is given by

$$\frac{\partial p}{\partial z} = G_p = \frac{fd}{z^2} \quad (3)$$

This shows that ranging accuracy, for a given image resolution, is proportional to source/detector separation and focal length, and decreases with the inverse square of range. In a scanned ranging system, there is an additional effect on ranging accuracy developed by the error in measurement of the projection angle. From (1) we have

$$\frac{\partial \theta}{\partial z} = G_\theta = \frac{d \cos^2 \theta}{z^2} \quad (4)$$

The effect on ranging of each of the geometrical/optical parameters of fig. 1 can be summarised as

- **Baseline:** A small baseline gives a compact sensor and ensures a good immunity to the missing parts problem. On the other hand, a large baseline improves range resolution.
- **Detector length and focal length:** A larger detector length can provide either a larger field of view or an improved range resolution or a limited degree of both, depending on the choice of focal length relative to the detector length. (A short focal length gives a large field of view at the expense of accuracy. A long focal length gives a good accuracy at the expense of field of view.) However, the geometric benefit from an increased detector length must be offset with increased sensor head size and a degradation of electrical characteristics. (For an LEP this would mean a lower bandwidth and a possible increase in both thermal and shot noise.)

To satisfy the depth of field requirements set out in section 3, whilst observing the above tradeoffs, we have chosen the following parameters for our camera head: baseline $d = 10\text{cm}$, focal length $f = 5\text{cm}$, and detector length $P = 1\text{cm}$. Our triangulation gain is thus given by $fd = 0.005\text{m}^2$. In order to use the whole of the detector length for the field of view the detection and projection axes are tilted towards each other by 8 degrees.

4.2 Synchronised scanning

Geometries based on synchronised scanning are employed in multi-dimensional ranging in order to maintain a more uniform triangulation geometry as the sensor scans over the scene. This uniformity minimises the tradeoffs that have to be made in the scanning geometry of the previous section. Oomen and Verbeek [7] introduced a lateral synchronization scheme in which the optical source scanned in a direction perpendicular to the detector field of view. We have adopted a longitudinal synchronization scheme, as suggested by Rioux [9], in which the scan direction is parallel to the detector field of view. The basic geometry of longitudinal synchronised scanning is schematically illustrated in fig. 2. In this geometry, the scanned beam is tracked by an imaging mirror so that the angular separation

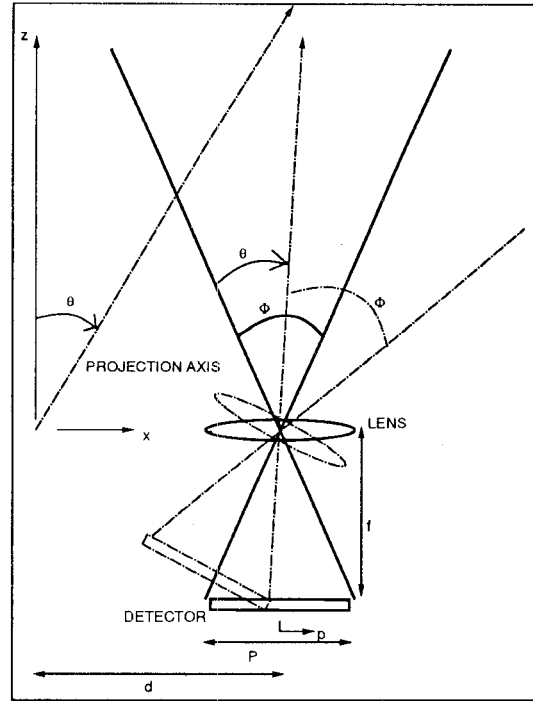


Figure 2: Schematic synchronised scanning geometry

between the projection and the detection axes remains constant. (Note that it is more difficult to keep the triangulation baseline constant over the scanning range because of a finite imaging mirror, imaging lens separation.) This means that the field of view of the detector rotates with the projection angle and that, to a first approximation, the scanning motion is subtracted from the image of the projected beam. Thus, the position of the image on the detector is much more dependent on range than on projection angle and nearly the whole of the detector length can be used to monitor range.

Simple geometrical analysis applied to this scheme yields

$$z = \frac{fd}{p} \cos^2 \theta + \frac{d}{2} \sin 2\theta \quad (5)$$

and x is again given by (2). The effects of image resolution and scan angle resolution on range accuracy can be described by the equations

$$G_p = \frac{fd \cos^2 \theta}{z^2} \quad (6)$$

$$G_\theta = \frac{1}{d \cos 2\theta - 2z \tan \theta} \quad (7)$$

Benefits of this geometry include

- Reduced susceptibility to angular error in scanning (7) as compared to a conventional geometry (4).
- Focal length can be adjusted to trade off resolution and depth of field (z range), as in a conventional geometry, but now there is no reduction in field of view (x range), since

this is dependent mainly on the angle over which scanning takes place. This means that there is no limitation in the aspect ratio of the viewing area.

- Ambient light immunity is improved, because the field of view rotates with the projection angle.

For our obstacle avoidance sensor, the basic triangulation parameters given at the end of the previous subsection are embedded in a synchronised scanning camera head.

5 The lateral-effect photodiode

Lateral-effect photodiodes (LEPs), also known as position sensing detectors (PSDs), are less well known in the robotics community than CCD sensors. This section is used to summarize their operation and characteristics before a qualitative comparison with triangulation based CCD sensors is made in the following section.

The LEP is constructed from a slice of silicon with P and N doped layers forming a PN junction. Charge carriers are generated by light impinging on the device, are separated in the depletion region, and are distributed to the electrodes at either end of the device. Since the device has uniform resistivity in the implanted layers, photocurrent is divided according to the position of the centroid of light intensity. Thus the position of the light centroid relative to the centre of the device is

$$p = \frac{I_1 - I_2}{I_1 + I_2} \left(\frac{P}{2}\right), \quad \left\{-\frac{P}{2} \leq p \leq +\frac{P}{2}\right\} \quad (8)$$

Important characteristics of an LEP are:

- *Spectral response:* A typical response would be from 400-1100 nm, peaking between 900 and 1000 nm.
- *Frequency response* For an LEP, bandwidth is mainly limited by the resistance and capacitance of the device. A typical 1-D detector that we have been evaluating has an active area of 10x2mm: R= 50kΩ, C=15pF which gives a bandwidth of 2MHz.
- *Image position resolution*
Position resolution of the centroid of image intensity is a function of detector length and the signal to noise ratio of the detector and signal processing electronics.
- *Detector noise*
Detector noise is the rms summation of the shot noise of the dark current (reverse bias saturation current) and thermal noise from the resistive layer. In small area (1-D) LEPs thermal noise usually dominates, whereas in larger area(2-D) LEPs, shot noise dominates.

6 CCD/LEP comparison

In a CCD, image resolution is dependent on the pixel density. If pixel size is small compared to the image size, sub-pixel accuracy may be obtained by fitting a curve through a set of pixel intensity values. This, however, increases the cost and complexity of analysing the data. In contrast, an LEP is a continuum, and image position is derived from the normalised

difference in current signals at the terminals of the device. The resolution of this image position is a direct function of signal to noise ratio over the measurement bandwidth. This implies that at short ranges or with high power light sources, when the image irradiance is high, an LEP will outperform a CCD. At longer ranges and lower power light sources, a CCD will resolve image position more accurately. For a given application, we must determine the range above which a CCD can improve on LEP resolution in order to make a sensible choice of image sensor.

In addition to a comparison of image resolution, bandwidth must be considered (although the two are related through signal averaging). In CCD based triangulation, measurement is restricted to frame rate, which, typically, may be 10kHz. For an LEP, measurement bandwidth is only limited by the capacitance and resistance of the device. For a 10x2mm 1-D LEP, this is around 2MHz although, in practice, measurement bandwidth in the signal processing circuitry must be restricted in the interests of signal to noise ratio.

In addition to a comparison of image position resolution, the following points must be considered when comparing the two devices

- The segmented structure of a 2-D CCD provides us with the option of scanning a stripe of light to make n range readings per frame on a profile perpendicular to the sweep direction. LEPs (1-D and 2-D), however, can only employ flying-spot coverage.
- The LEP is much more insensitive to badly collimated light sources and defocusing with range variations as compared with the CCD, since it integrates light intensity over its surface to provide image position. A CCD based system can combat these problems with peak detection circuitry and Scheimflug geometries.

7 Optical sources and eye-safety

7.1 Laser diodes or LEDs?

The coherence of the laser allows us to collimate into a very narrow, parallel beam of light, bringing the advantages of specific localised probing of the environment and a small image size. In addition, their spectral purity allows the use of very narrow band optical filters to reject ambient light. The great problem of a laser, when projected into an open environment, is the eye safety problem, which sets an upper limit on the power output. This limitation is more detrimental to LEP based sensors than to CCD based sensors.

A light emitting diode (LED) is an incoherent light source which emits over a range of wavelengths. Although the refractive index of glass varies with wavelength, the main problem in collimating an LED lies with its incoherence. Collimation is particularly difficult with high power LEDs since they emit over a large area. Poor collimation brings the disadvantages of a large "footprint" of light which may straddle and blur features (edges, corners, etc) in the environment, cumbersome beam scanning, and a large image size. The great advantage of an LED is that there are no problems with eye safety. High

power LEDs may be employed which eliminates the usual signal to noise problem encountered with LEPs.

Preliminary experiments have shown that for the one-dimensional measurement of range, an LED/LEP based system can perform well. For multidimensional (scanned) ranging, particularly using CCDs, a collimated (or fanned) laser beam is the only realistic choice of optical source.

Often, image sensors are most responsive to infra-red frequencies, however, for ease of use and for purposes of safety, we have chosen a visible laser diode as our optical source.

7.2 Maintaining class I laser hazard

For our sensor, we wish to maintain a class I (if scanning is guaranteed) or class II (if scanning is not guaranteed) laser hazard classification so that the vehicle workspace is always accessible to operators. This is in conflict with the laser output requirement for high accuracy, since accuracy degrades with decreasing signal to noise ratio. In designing a sensor, the measurement bandwidth must be able to support a scanning frequency which is high enough to make a given laser power safe, yet at the same time the laser power must be high enough to give a reasonable accuracy at the measurement bandwidth.

Class I status can be given to higher power lasers if we can guarantee laser scanning. Given that we can guarantee that the laser will be scanning over a minimum angle and above a minimum frequency, and given that there is a minimum accessible distance for a naked eye staring into the sensor aperture, the maximum laser output power can be calculated in order to maintain a class I hazard status. In order to permit the use of lasers that are more powerful than 1mW, a laser interlock mechanism has been developed which consists of a 'sweet spot' LED directed into the scanning mirror, the reflected beam of which scans across a monitor LEP. If the frequency or amplitude of the monitor LEP image position signal falls below hardware set minima, then the laser is shut down.

8 Predicted Accuracy of an LEP Based Rangefinder

The discrete nature of a CCD and its superior noise performance, as compared to an LEP, mean that image resolution in a ranging system is more uniform over the sensor depth of field. However, LEPs are cheaper than CCDs and it is much simpler to extract image position from the sensor. In this section, we generate theoretical performance curves for an LEP based sensor by varying range and measurement bandwidth. These are normalised to projected power and compared to real data. Using this analysis we can determine whether we can expect satisfactory performance from an LEP based system whose depth of field ranges from 0.4-2.5m. In the analysis, the effect of image resolution only is considered.

Image resolution for an LEP is

$$\Delta p = \frac{P}{2 \frac{I_s}{I_n}} \quad (9)$$

where P is the detector length and $\frac{I_s}{I_n}$ is the signal current to noise current ratio of the detection.

If we assume that the projected spot is small enough and distant enough to be treated as a point source and that purely lambertian scattering occurs in the scene, then the total signal current I_s at range r , for laser power P_t , can be approximated by [5]

$$I_s = \frac{T_1 T_2 \rho A R_\phi \cos \theta_d}{2\pi z^2} P_t \quad (10)$$

where, for our camera head design, the light collecting aperture $A = 6\text{cm}^2$, transmission in the light projection optics $T_1 = 0.7$, and transmission in the light collecting optics $T_2 = 0.8$. Also, we will assume an average scene reflectivity $\rho = 0.7$, and a zero angle of scene surface relative to the detector, $\theta_d = 0$.

Noise current (I_n) in (9) is calculated from the detector/preamplifier noise density over the measurement bandwidth. The total detector noise density is the rms summation of shot and thermal noise. For our device, dark current $I_d = 100\text{nA}$, $R_s = 50\text{k}\Omega$ and assuming $T = 298\text{K}$:

$$i_{nd} = \sqrt{2eI_d + \frac{4kT}{R_s}} = 0.6pAH z^{-\frac{1}{2}} \quad (11)$$

Note that we have ignored shot noise due to the signal current which is negligible compared to detector thermal noise in the rms summation of noise sources. Preamplifier noise, including feedback resistor noise ($R_f = 1\text{M}\Omega$) is given as:

$$i_{na} = \sqrt{i_{na}^2 + \frac{e^2 n_a}{R_s} + \frac{4kT}{R_f}} = 0.237pAH z^{-\frac{1}{2}} \quad (12)$$

Calculating the rms of (11) and (12) gives the total current noise density (I_n) for the detector-preamplifier combination as $0.645pAH z^{-\frac{1}{2}}$. This figure, along with (10) allows us to calculate image resolution from (9) for any range or measurement bandwidth. Image resolution can then be projected to range resolution through the triangulation gain expressed in (3). Thus we have an equation for scene resolution:

$$\Delta z = \frac{k}{P_t} B^{-\frac{1}{2}} z^4 \quad (13)$$

where

$$k = \frac{\pi I_n P}{fd T_1 T_2 \rho R_\phi A \cos \theta_d} \quad (14)$$

Substituting our specifications and assumed values, $k = 3.47 \times 10^{-8} \text{WH} z^{-\frac{1}{2}} \text{m}^{-3}$. The specification of section 3 suggested that a complete scan (1000 measurements) should take place every 0.1-1s. Thus by varying range over 0.4-2.5m and bandwidth from 1-10kHz, performance curves can be generated from (13). Curves for a projected power of 1mW are given in fig. 3.

At the maximum bandwidth required and at the maximum range, fig 3 illustrates that an average projected laser power of 5mW is required in order to maintain the 1% accuracy specified in section 3. Without the use of a laser shutdown mechanism, 1mW is the class II eye safety limit. In this case, fig 3 shows that the sensor bandwidth has to be limited to 1kHz in order to maintain reasonable accuracy over the whole depth of field. Here, we should note that errors due to angular measurement

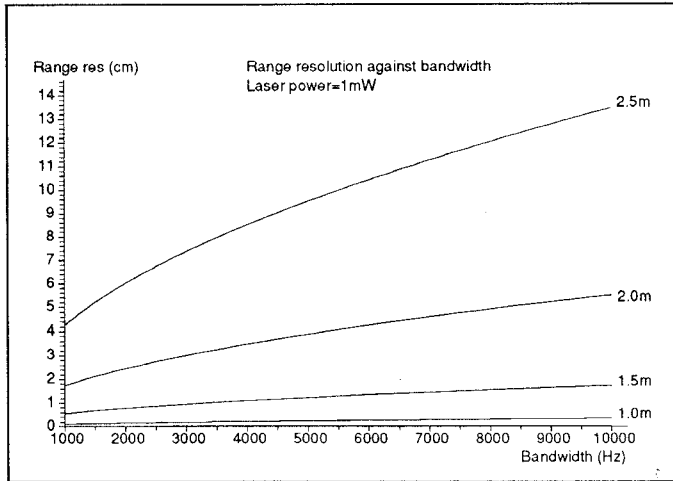


Figure 3: Range resolution against bandwidth

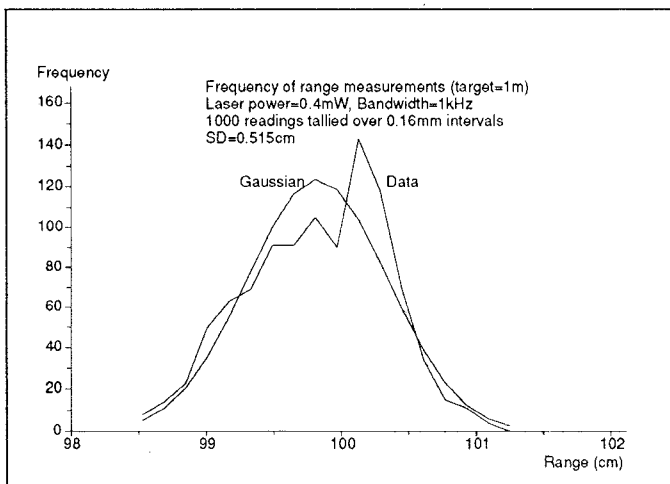


Figure 4: Distribution of range measurements for a 0.4mW laser

also contribute to the total error of a scanning sensor. For our sensor, scan angle is repeatable to 0.2mrad. Equation (7) shows that ranging error due to scan angle resolution is small compared to ranging error due to a limited position resolution.

Our sensor was tested with the scanner switched off and a 0.4mW (eye safe) laser was used to test ranging accuracy. A sample result for a target at 1m is shown in fig. 4. The measured standard deviation is approximately 5mm whereas theory predicts an accuracy of approximately 3mm. We have attempted to approach white noise levels through the use of laser modulation and synchronous (lock-in) detection techniques. Fig. 4 demonstrates a range resolution of the same order of magnitude as theory predicts. Note that the skew of the results away from the Gaussian is due to the non-linearity of the calibration.

9 Conclusions

We have discussed active triangulation rangefinder design with a view to implementing a short-medium (0.4-2.5m) range obstacle avoidance sensor for mobile robots. This discussion has shown the implications of choosing various configurations in terms of accuracy and bandwidth. We have analysed the performance of an LEP based sensor, and shown that a real sensor can be built which achieves a performance close to theoretical prediction. This sensor has been shown to have characteristics appropriate for realising a manoeuvring capability for a mobile robot.

References

- [1] Jarvis R. A. A perspective on range finding techniques for computer vision. *IEEE trans. on Pattern Analysis and Machine Intelligence*, PAMI-5(2):122-139, 1983.
- [2] Rioux M. Blais F. and Domey J. Optical range image acquisition for the navigation of a mobile robot. In *Proc. 1991 IEEE Int. Conf. on Robotics and Automation*, pages 2574-2580, 1991.
- [3] Lo H.R. Blake A., McCowen D. and Konash D. Epipolar geometry for trinocular active range sensors. In *Proc. British Machine Vision Conf.*, 1990.
- [4] Bastuscheck C.M. Techniques for real-time generation of range images. In *Proc. IEEE CVPR*, pages 262-268, 1989.
- [5] Svetkoff D.J. Towards a high resolution, video rate, 3d sensor for machine vision. In *SPIE 728*, pages 216-226, 1986.
- [6] Miller G.L. and Wagner E.R. An optical rangefinder for autonomous robot cart navigation. In *SPIE 852*, pages 122-134, 1987.
- [7] Oomen G.L. and Verbeek W.J.P.A. A real-time optical profile sensor for robotic arc welding. In *SPIE 449*, pages 62-71, 1984.
- [8] Everett H.R. Survey of collision avoidance and ranging sensors for mobile robots. *Robotics and Autonomous Systems*, 5:5-67, 1989.
- [9] Rioux M. Laser rangefinder based on synchronised scanners. *Applied Optics*, 23(21):3837-3844, 1984.
- [10] Livingstone F. R. and Rioux M. Development of a large field of view 3-d vision system. In *SPIE 665*, pages 188-194, 1986.
- [11] Reid G. T. and Rixon R. C. Stripe scanning for engineering. *Sensor Review*, 8(2):67-71, 1988.